SCIENCE CHINA
Life Sciences

FROM CAS & CAE MEMBERS
•RESEARCH PAPER•

June 2022 Vol.65 No.6: 1075–1090
https://doi.org/10.1007/s11427-021-2055-x

Pathogen-associated T follicular helper cell plasticity is critical in anti-viral immunity

Han Feng[1], Xiaohong Zhao[1], Jenny Xie[2], Xue Bai[1], Weiwei Fu[1,3], Hairong Chen[4], Hong Tang[4,5,6], Xiaohu Wang[1] & Chen Dong[1,7*]

[1]*Institute for Immunology, Tsinghua University, Beijing 100084, China;*
[2]*Discovery Immunology, Bristol Myers Squibb, Princeton NJ 08543, USA;*
[3]*Department of Gastroenterology, Peking University Third Hospital, Beijing 100191, China;*
[4]*CAS Key Laboratory of Infection and Immunity, Institute of Biophysics, Chinese Academy of Science, Beijing 100101, China;*
[5]*CAS Key Laboratory of Molecular Virology and Immunology, Institute Pasteur of Shanghai, Chinese Academy of Sciences, Shanghai 200025, China;*
[6]*Pasteurien College, Suzhou University, Suzhou 215123, China;*
[7]*Shanghai Immune Therapy Institute, Shanghai Jiao Tong University School of Medicine Affiliated Renji Hospital, Shanghai 200127, China*

Received August 10, 2021; accepted September 26, 2021; published online March 2, 2022

T follicular helper (Tfh) cells are critical in providing help for B cells in the germinal center reaction. Tfh cell plasticity, especially with regard to their expression of effector Th cytokines, has been described, but lacks in-depth analysis with genetic approaches. In this study, we systemically compared transcriptomic profiles of Tfh cells derived from various types of immune responses and found gene clusters corresponding to effector Th cells were differentially induced in response to pathogens or immune responses. Of special interest, a subset of Tfh cells producing IFN-γ was generated in an influenza virus infection, partially dependent on the innate cytokine IL-12. Lineage-tracing mouse model revealed unique developmental regulation of IFN-γ^+ Tfh cells, while selective ablation of these cells impaired the induction of IgG2c$^+$ germinal center B cells and the control of influenza infection. These results indicate that pathogen-associated Tfh cell plasticity is necessary for host immunity, which has implications in vaccine design.

T follicular helper (Tfh) cell, plasticity, influenza infection, IFN-γ, IgG2

Citation: Feng, H., Zhao, X., Xie, J., Bai, X., Fu, W., Chen, H., Tang, H., Wang, X., and Dong, C. (2022). Pathogen-associated T follicular helper cell plasticity is critical in anti-viral immunity. Sci China Life Sci 65, 1075–1090. https://doi.org/10.1007/s11427-021-2055-x

INTRODUCTION

Antibody is essential for host protection against foreign pathogens; defects in antibody production result in susceptibility to bacterial, viral and parasitic infections. Based on the heavy chains, antibodies are classified into five major classes or isotypes, i.e., IgA, IgD, IgE, IgG and IgM. IgG in mouse can be further divided into IgG1, IgG2a/c, IgG2b and IgG3 subclasses (Xu et al., 2012). Depending on the subclass, IgG antibodies are highly effective in opsonizing and neutralizing pathogens as well as in activating the complement system, while IgA and IgE have almost no ability to activate complement (Ward and Ghetie, 1995). Moreover, different IgG subclasses have different binding affinities for Fc receptors (FcRs) expressed on immune effector cells. IgG1 does not bind to FcγRIV or FcγRI, but functions via FcγRIII. In contrast, IgG2a in BALB/c and IgG2c in C57BL/6 mice additionally bind to high-affinity FcγRI and FcγRIV, and activate complement better than IgG1 (Coutelier et al., 1987; Huber et al., 2006; Sangster et al., 2000; Živković et al.,

*Corresponding author (email: chendong@tsinghua.edu.cn)

2018).

Antibody isotype switching in B cells is dependent on the nature of antigen, as well as "help" from T cells. IL-21, predominantly produced by T follicular helper (Tfh) cells, is critical in the production of antigen-specific antibody, especially of the IgG1 isotype; deletion of *Il21r* dampened IgG1 while increasing IgE levels (Ozaki et al., 2002; Suto et al., 2002). IL-4, on the other hand, is essential for IgE production and is also important in IgG1 class switching (Gowthaman et al., 2019; Wu and Zarrin, 2014). Double deficiency in IL-4 and IL-21 eliminated IgG1 and IgE isotypes (Ozaki et al., 2002), indicating overlapping regulation of IgG1 production by IL-21 and IL-4. On the other hand, IFN-γ selectively induces IgG2 antibody, which is the predominant protective neutralizing antibody isotype in murine viral infections (Miyauchi et al., 2016; Snapper and Paul, 1987). TGF-β mediates the IgG2b and IgA class switch (Park et al., 2005).

The Tfh cell is specialized in delivering help to B cells and is required for germinal center reactions. Originally defined by the expression of CXCR5, which facilitates Tfh cell migration into B cell follicles (Ansel et al., 1999; Breitfeld et al., 2000; Kim et al., 2001; Schaerli et al., 2000), Bcl-6 was subsequently determined as the first lineage-specific transcription factor in Tfh cells (Johnston et al., 2009; Nurieva et al., 2009; Yu et al., 2009). Inactivation of the *Bcl6* gene in $CD4^+$ T cells impaired Tfh cell formation and the germinal center response. Tfh cells are essential in generating high-affinity antibody through the germinal center reaction (Crotty, 2019; King et al., 2008; Vinuesa et al., 2016), likely via providing the CD40L and IL-21 signals to promote B cell proliferation and differentiation (Glatman Zaretsky et al., 2009; Linterman et al., 2010; Xu et al., 1994; Zotos et al., 2010). Cytokines released by T cells together with CD40L further induce Activation-induced Cytidine Deaminase (AID) expression in B cells, which promotes class-switch DNA recombination of the immunoglobulin heavy chain, thus give rise to different antibody isotypes (Glatman Zaretsky et al., 2009; King and Mohrs, 2009; Reinhardt et al., 2009), as well as somatic hypermutation of Ig V genes.

Although originally reported to lack the expression of signature cytokines and transcription factors found in Th1, Th2 and Th17 cells (Nurieva et al., 2008), Tfh cells have also been reported in the literature with different phenotypic and functional features. Based on the expression of CXCR3 and CCR6, Tfh cells in human peripheral blood, although they lack Bcl6 expression, were subdivided into $CXCR3^+CCR6^-$ Tfh1, $CXCR3^-CCR6^-$ Tfh2 and $CXCR3^-CCR6^+$ Tfh17 cells with distinct capacities to help B cells *in vitro* (Morita et al., 2011; Schmitt et al., 2014). The blood $CXCR3^+CXCR5^+$ $ICOS^+$ Th cells positively correlate with the induction of protective antibody responses upon seasonal flu vaccination (Bentebibel et al., 2013), though their functions are still controversial. During chronic SIV infection, a large fraction of GC-Tfh cells expresses CXCR3 and IFN-γ, associated with increased IgG1 production, and may serve as viral reservoirs (Velu et al., 2016). One recent work showed that in a ZIKA infection model in the presence of IFNRA blockade, Th1-like Tfh cell population was induced, which was required for the virus-specific IgG2c class switching and promoted plasma cell differentiation (Liang et al., 2019). However, the ontogeny of those cells and the relationship between Tfh cells and Th1 cells remains unclear. On the other hand, sequentially acquired IL-4 expression by GC-Tfh cells, together with IL-21 expression, was reported to regulate IgG1 production and antibody-secreting plasma cell differentiation in *Nippostrongylus brasiliensis*-infected mice (Weinstein et al., 2016). Recently, Tfh13 cells, which produce IL-13 along with IL-4, were identified and shown to be necessary for anaphylactic IgE production in response to allergens (Gowthaman et al., 2019). Taken together, all of the above data suggest the existence of Tfh cell heterogeneity and/or plasticity. However, whether different subtypes of Tfh cells are present in all immune responses or, if instead, they display different features depending on the immune context, has not been resolved, especially by use of genetic approaches.

To understand whether and how Tfh cells regulate B-cell production of IgG isotypes in different immune responses, we performed RNA sequencing on Tfh cells generated in a variety of infection and immunization models. Tfh cells were found to exhibit distinct phenotypes depending on the immune context. Moreover, we found an IFN-γ-secreting Tfh cell population in viral and bacterial infections that is regulated by IL-12 signaling. Fate-mapping mouse model reveals IFN-$\gamma^{+/-}$ Tfh cells are generated in parallel, and specific elimination of IFN-γ^+ Tfh cells during influenza infection dampened anti-viral antibody production, especially of the $IgG2^+$ germinal center B cells, resulting in susceptibility to influenza infection. Our data indicate Tfh cell plasticity depending on the nature of the infection, which has implications in the rational design of vaccines.

RESULTS

Tfh cells exhibit distinct gene expression features in different immune responses

To systemically analyze and compare Tfh cells in different types of immune responses, we used $Bcl6^{RFP}\times Foxp3^{GFP}$ mice (Fontenot et al., 2005; Liu et al., 2012) to isolate *bona fide* GC-Tfh cells based on the $CXCR5^+Bcl6^+Foxp3^-$ gating (Figure 1A) from Peyer's patches at steady state, as well as draining lymph nodes (dLNs) in keyhole limpet hemocyanin (KLH)-immunized, influenza virus A/Puerto Rico/8 (PR8, H1N1)-infected, *S. mansoni* soluble egg antigen (SEA)-

treated, and experimental Sjögren's syndrome (ESS)-induced mice. RNA sequencing analysis followed by transcriptome comparisons were performed on these various types of Tfh cells. As expected from previous literature (Liu et al., 2012), genes including *Il21*, *Cxcr5*, *Tox*, *Sh2d1a*, *Bcl6*, *Dnase1l3*, *Slamf6*, *Fas*, *Id3*, *Tspan32*, *Cd160*, *Cd200*, *Btla*, *Cd27*, *Cd69*, *Egr2* and *Egr3* were highly expressed among all Tfh cells, when compared to non-Tfh cells. In total, there were 450 genes sharing similar expression patterns in Tfh cells, which identifies a core module of the Tfh cell transcriptional signature (Figure 1C). Further analysis revealed that these commonly expressed genes in Tfh cells are highly enriched in pathways associated with T cell activation, B cell activation and regulation, and immunoglobulin production (Figure 1D). Principal component analysis (PCA) also showed distinct transcriptional characteristics in Tfh cells from these models. Moreover, Tfh cells derived from the KLH immunization and ESS models shared more transcriptional similarity, compared with other models, with relatively higher expression of *Icos*, *Tcf7*, *Il6ra* in both (Figure 1B and E). This could possibly be due to the use of complete Freund's adjuvant (CFA) in both models, suggesting that innate immunity has a strong influence on the transcriptional program of Tfh cells. Of note, Tfh cells generated during influenza virus infection elicited upregulated expression of *Ifng*, together with increased *Tbx21*, *Il10*, *Cxcr3*, *Fos*, *Pdcd1*, *Ascl2* expression compared to the other models. In contrast, transcription of *Il4* and *Il5* was significantly elevated in the SEA immunization model (Figure 1E).

These data indicate that Tfh cells, though they share a core transcriptional module, preferentially express certain Th-related genes depending on the nature of the immune responses, a phenotype likely imprinted by the innate immune reaction.

Specific induction of IFN-γ$^+$ Tfh cells during viral infection

Tfh cells have been shown to be important in influenza infection (Liu et al., 2014). Although IFN-γ$^+$ Tfh cells represent a unique feature of viral and bacterial infection, they constituted only a small fraction of total Tfh cells. To further characterize IFN-γ-expressing Tfh cells, we utilized *Bcl6*^{RFP}×*Ifng*^{YFP} mice. Consistent with RNA sequencing results and FACS staining, approximately 20%–30% of CXCR5$^+$RFP(Bcl6)$^+$ Tfh cells in the lung draining lymph nodes during influenza infection were YFP(IFN-γ)$^+$ (Figure 2A and E). In response to *L. Monocytogenes* infection, IFN-γ$^+$ Tfh cells were detected at levels comparable to influenza infection. In contrast, Tfh cells exhibited only very modest YFP expression in Peyer's patches at the resting state, with no expression detected after KLH or SEA immunization (Figure 2E). During influenza infection, approximately 10%–15% activated CD4$^+$ T cells were YFP$^+$RFP$^+$ (Figure 2B). However, there were no natural killer (NK) cells, macrophage, dendritic cells, B cells or CD8$^+$ T cells co-expressing IFN-γ and Bcl6 upon influenza challenge (Figure 2C).

We also observed specific cellular localization of YFP$^+$ RFP$^+$ CD4$^+$ T cells inside of the PNA$^+$IgD$^-$ GC areas of draining lymph nodes at D9 post influenza infection (Figure 2D). By contrast, YFP single positive CD4$^+$ T cells, likely Th1 cells, were found outside of follicles. These results suggest a role of IFN-γ-expressing Tfh cells in regulating GC responses.

Next, we compared the transcriptional profiles of IFN-γ$^+$ and IFN-γ$^-$ Tfh cells by RNA sequencing. A total of 279 genes were found significantly (>2-fold) upregulated in IFN-γ$^+$ Tfh cells and 252 genes were downregulated. By comparison with Th1 and Tfh cells generated during viral infection, we found that Th1-related and cytotoxicity-related genes, including *Ccl3*, *Il12rb2*, *Ccl4*, *Cxcr6*, *Zeb2*, *Bhlhe40*, *Ifng*, *Il18rap*, *Tbx21*, *Ccr2*, *Prdm1*, *Gzmb* and *Runx2* were highly expressed in IFN-γ$^+$ Tfh cells (Figure S1A and B in Supporting Information), while several Tfh signature genes like *Btla*, *Tox* and *Pou2af1* were decreased in expression compared to IFN-γ$^-$ Tfh cells. The expression of *Icos* was higher in IFN-γ$^+$ Tfh cells. Interestingly, expression of several memory-related genes, including *Sell*, *Ccr7* and *Klf9*, was increased in IFN-γ$^-$ Tfh cells. Of note, expression of *Cxcr3*, previously identified as a Th1-like Tfh cell marker in human peripheral blood (Ma and Deenick, 2014; Morita et al., 2011), did not correlate with that of *Ifng* in Tfh cells during influenza infection (Figure S1A in Supporting Information), suggesting that CXCR3 may not be involved in regulating the localization of these cells. Considering this, IFN-γ$^+$ Tfh cells in our flu model may not be exactly the same population as the previously reported CXCR3$^+$ Tfh or Tfh-like population in human or mouse (Obeng-Adjei et al., 2015; Ryg-Cornejo et al., 2016; Velu et al., 2016; Velu et al., 2018).

Gene set enrichment analysis (GSEA) using published transcription datasets revealed that IFN-γ$^+$ Tfh shared more similar features with Th1 cells rather than Tfh cells in LCMV infection (Shaw et al., 2016) (Figure S1C in Supporting Information). Pathway analysis of upregulated genes in IFN-γ$^+$ Tfh cells indicated that they were enriched for genes related to cellular cytotoxicity and B cell responses (Figure S1D in Supporting Information), suggesting bifunctional characteristics of these cells. To further validate the differentially expressed genes between these two subsets, we examined T-bet, TOX, BLIMP1 and BCL6 protein expression in IFN-γ$^+$ Tfh cells and IFN-γ$^-$ Tfh cells by flow cytometry. Consistent with mRNA expression, IFN-γ$^+$ Tfh cells showed increased T-bet and BLIMP1 expression, but similar levels of BCL6 expression, compared to IFN-γ$^-$ Tfh cells. However, unlike

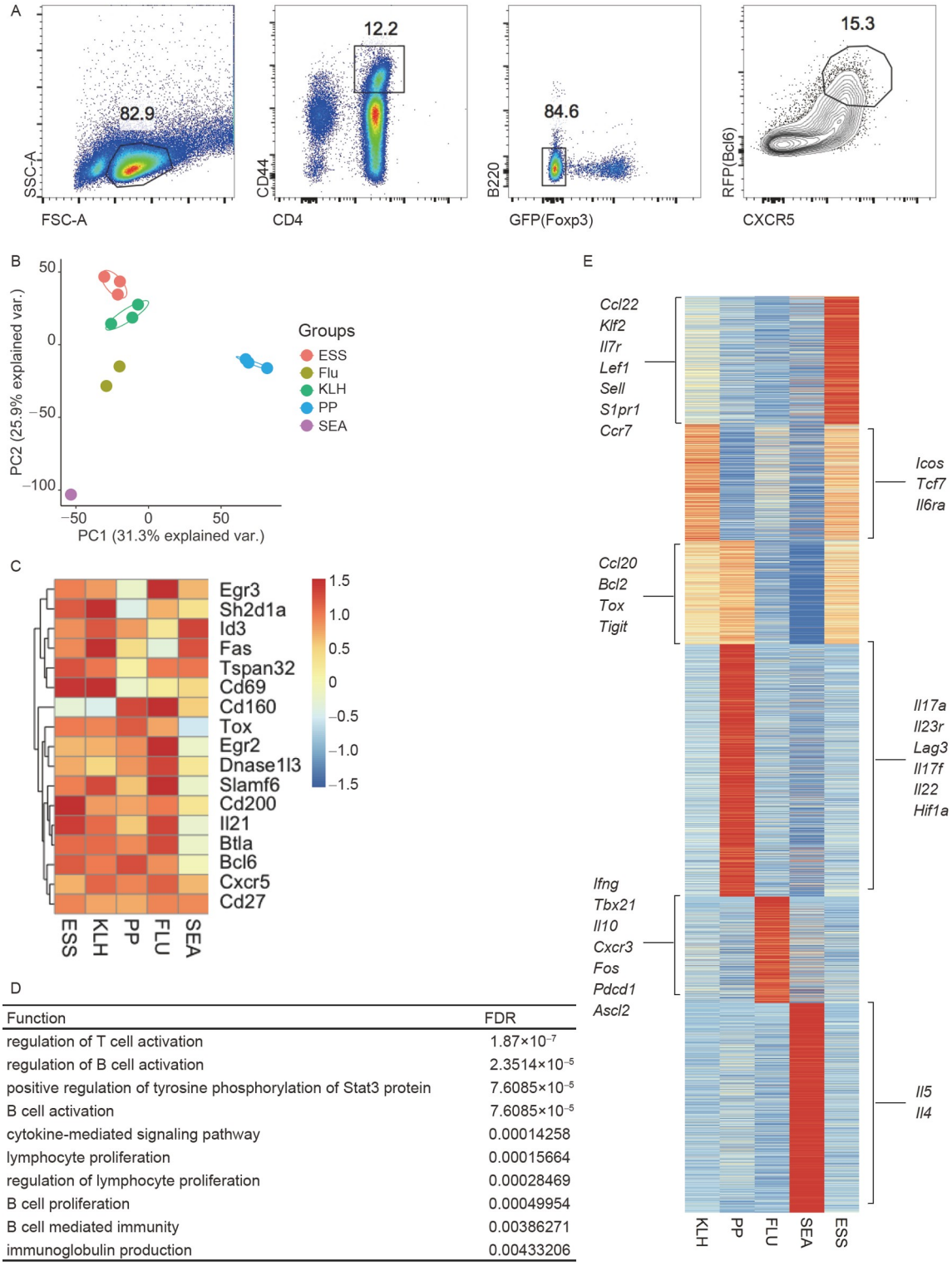

D

Function	FDR
regulation of T cell activation	1.87×10^{-7}
regulation of B cell activation	2.3514×10^{-5}
positive regulation of tyrosine phosphorylation of Stat3 protein	7.6085×10^{-5}
B cell activation	7.6085×10^{-5}
cytokine-mediated signaling pathway	0.00014258
lymphocyte proliferation	0.00015664
regulation of lymphocyte proliferation	0.00028469
B cell proliferation	0.00049954
B cell mediated immunity	0.00386271
immunoglobulin production	0.00433206

Figure 1 Tfh cells exhibit distinct transcriptional profiles in different immune contexts. A, Representative example of gating strategy used to isolate GC-Tfh ($CD4^+CD44^{hi}CXCR5^+RFP^+GFP^-B220^-$) cells for bulk RNA sequencing. B, PCA of transcripts in five indicated mouse models. C, Heatmap of commonly expressed genes (FPKM>5) in 5 models compared to non-Tfh samples (fold change>2, FDR<0.01). D, Pathways enriched in commonly expressed genes. E, Heatmap of differentially expressed transcripts (fold change>2, FDR<0.01) among different models. Selected genes were highlighted in the heatmap.

RNA-seq result, TOX expression was similar, even higher in IFN-γ^+ Tfh cells (Figure S1E in Supporting Information). These results indicate that IFN-γ^+ Tfh cells have increased expression of Th1-associated genes, but maintain similar expression in Tfh related molecules. Moreover, gene set enrichment analysis also indicated that IFN-γ^+ Tfh cell

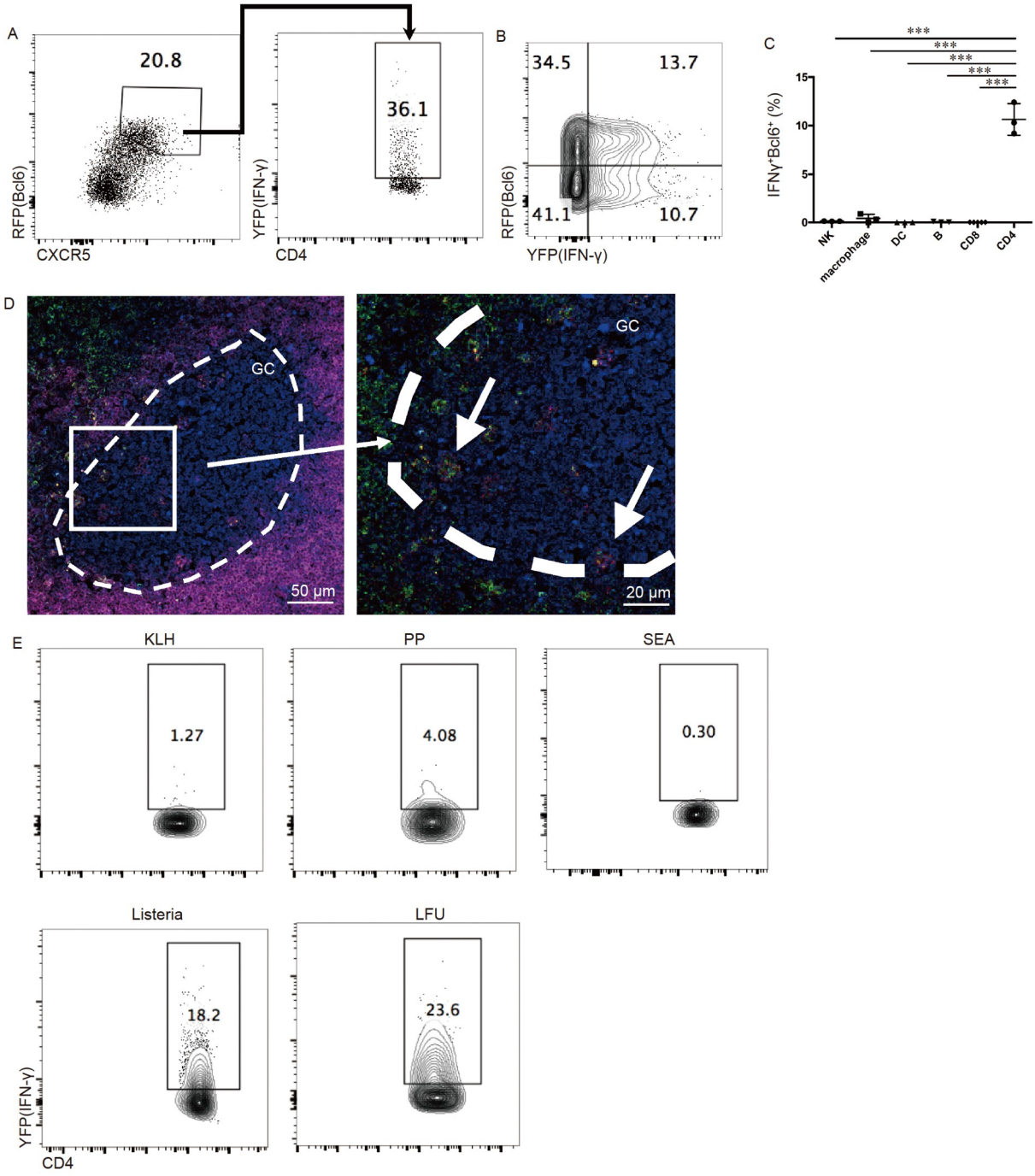

Figure 2 Specific induction of IFN-γ^+ Tfh cells during viral infection. The *Ifng*^{YFP}×*Bcl6*^{RFP} reporter mice were intranasally infected with H1N1 PR8 influenza virus and analyzed 9 d later. A, Representative flow cytometric images of *Ifng*-YFP reporter expression in CXCR5$^+$RFP$^+$ Tfh cells and (B) YFP$^+$RFP$^+$ cells (gated on CD4$^+$CD44^{hi}). C, Statistics of YFP$^+$RFP$^+$ populations in NK cells (gated on CD3$^-$NK1.1$^+$), macrophages (F4/80$^+$), dendritic cells (MHCII$^+$CD11c$^+$CD11b$^+$), B cells (CD19$^+$B220$^+$), CD8$^+$ T and CD4$^+$ T cells. D, Representative immunofluorescence images of PNA (blue), YFP (green), RFP (red), IgD (violet) staining in the frozen sections of lung draining lymph nodes. E, Representative YFP expression in Tfh cells from Peyer's patches at steady state, as well as dLNs in KLH immunized, H1N1 PR8 infected and SEA immunized or spleen in *Listeria Monocytogenes* infected *Ifng*^{YFP}×*Bcl6*^{RFP} reporter mice. Data are shown as mean±SD; two-tailed *t*-test; *, P<0.05; **, P<0.01.

highly expressed apoptosis-related molecules (Figure S1F in Supporting Information), which imply that they might undergo apoptosis rather than differentiation into memory cells, after peak of the immune response.

Reduced capacity of inactivated influenza virus in inducing protective humoral immunity

Vaccination is the most effective way to prevent the spread of influenza infection. We thus compared the development of

IFN-γ^+ Tfh cells during infection by natural H1N1 PR8 and vaccination with virus chemically inactivated using a previously described method with modifications (Miyauchi et al., 2016). Natural infection with influenza virus induced preferentially expression of Bcl6 and IFN-γ in $CD4^+$ cells in lung dLNs and lung tissue, respectively, likely due to the differences in cytokine environments and cellular distributions between lymph nodes and lung tissues (Figure 3A and B). $CXCR5^+Bcl6^+$ Tfh cells were very limited in lung tissue compared to lung dLNs, mainly due to lack of classical GC structure in lung tissue. When we compared T cell phenotypes between natural virus and inactivated virus vaccination, although similar percentages of IFN-γ^+ CD4 T cells were induced by live virus infection and vaccination, IFN-γ^+Bcl6^+ double-positive cells as well as IFN-γ^-Bcl6^+ single-positive cells were not significantly induced in lung dLNs by vaccination (Figure 3A and B). Furthermore, GC B cells in lung draining lymph nodes were significantly decreased compared to live virus infection (Figure 3B). Moreover, IgG2c production by GC B cells in either dLNs or lung tissues was significantly decreased in vaccinated mice compared to infected mice (Figure 3C and D). These results suggest a reduced capacity of inactivated influenza virus in inducing protective immunity compared to live influenza

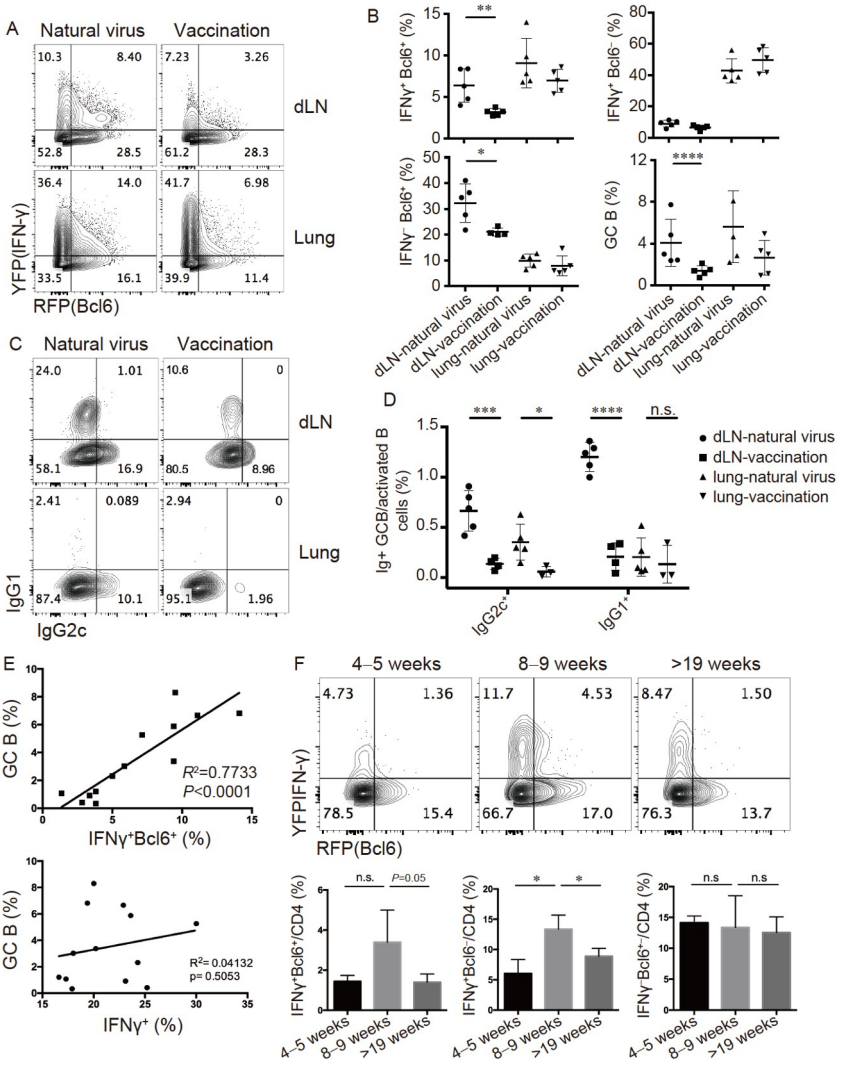

Figure 3 Inadequate induction of IFN-γ^+ Tfh cells by inactivated influenza virus vaccine. The *Ifng*^{YFP}×*Bcl6*^{RFP} reporter mice were either infected with live PR8 virus or immunized with inactivated virus (vaccination), and then sacrificed and analyzed on day 9 post infection, or on days as indicated. A, Representative flow images of *Ifng*-YFP and *Bcl6*-RFP expressions in $CD4^+CD44^{hi}$ T cells obtained from lung draining lymph nodes and lung tissues of *Ifng*^{YFP}×*Bcl6*^{RFP} reporter mice. B, Statistical analysis of IFN-γ^+Bcl6^+ $CD4^+$ T cells, IFN-γ^+Bcl6^- $CD4^+$ T cells, IFN-γ^-Bcl6^+ $CD4^+$ T cells and GC B cells (gating) obtained from lung draining lymph nodes and lung tissues of *Ifng*^{YFP}×*Bcl6*^{RFP} reporter mice. C, Representative flow images of IgG1 and IgG2c staining in GC B cells obtained from lung dLNs or lung tissues of the reporter mice. D, Statistical analysis of $IgG1^+$ or $IgG2c^+$ GC B cell percentages in total IgD^- activated B cells in lung dLNs or lung tissues. E, Correlation analysis of IFN-γ^+Bcl6^+ $CD4^+$ T cell or IFN-γ^+ $CD4^+$ T cell percentages with GC B cell percentages. F, Representative flow images (upper) and statistical analysis (below) of YFP^+RFP^+ cells in $CD4^+CD44^{hi}$ T cells in lung draining lymph nodes of *Ifng*^{YFP}×*Bcl6*^{RFP} reporter mice vaccinated at ages of 4–5, 8–9 or >19 weeks old. Data above are representatives of two independent experiments. Data are shown as mean±SD; two-tailed *t*-test; *, $P<0.05$; **, $P<0.01$; ***, $P<0.001$; ****, $P<0.0001$; n.s, no significance.

virus, especially in the Tfh compartment. Moreover, when we integrated the analysis on live influenza infection and inactivated influenza vaccination results, GC B cell development appeared to positively correlate with the percentages of IFN-γ^+Bcl6$^+$, but not total IFN-γ^+ CD4$^+$ T cells (Figure 3E). Furthermore, when we compared mice at different ages in terms of their responses to the inactivated influenza vaccination, IFN-γ^+Bcl6$^+$ and IFN-γ^+Bcl6$^-$ cell populations were both significantly decreased in juvenile (4 weeks) and elderly (>19 weeks) groups compared to mice of 8w, whereas similar frequencies of IFN-γ^-Bcl6$^+$ cells were identified in all three groups (Figure 3F). Thus, age may affect IFN-γ expression in T cells, which may underscore the differential efficacy of vaccine protection in humans (Flannery et al., 2019; Goodwin et al., 2006; Osterholm et al., 2012).

Innate signaling regulates the induction of IFN-γ^+ Tfh cells during influenza infection

Interleukin 12 is necessary for Th1 cell differentiation (Romani et al., 1997). Our RNA-sequencing result showed that *Il12rb2*, but not *Il23r*, gene expression was significantly increased in IFN-γ^+ Tfh compared to IFN-γ^- Tfh cells. Interestingly, the *Il12p40* (*Il12b*) gene was selectively and highly expressed in lung dLN cells during influenza infection, but not in draining lymph nodes after SEA immunization, KLH immunization or in Peyer's patches at the steady state (Figure 4A). *Il12p35* (*Il12a*) gene expression pattern was similar to that of *Il12p40*, although it was also highly expressed in the KLH immunization model (Figure 4A). We also compared *Il12* expression during live virus infection and vaccination. Although *Il12p40* showed similar expression levels between live virus and vaccine, *Il12p35* expression was significantly higher with live virus infection (Figure 4B). These data suggest that *Il12* is selectively expressed during influenza infection, which may impact the induction of IFN-γ^+Bcl6$^+$ cells. To further investigate the source of IL-12, we examined IL-12 expression in lung dLNs and lung-infiltrating cells through flow cytometry. Overall, CD11c$^+$ dendritic cells produced higher amounts of IL-12 compared to B220$^+$ B cells in both lung dLNs and lung tissue after influenza infection (Figure 4C). B cells barely produced IL-12 in draining lymph nodes, however, expressed elevated levels of IL-12 in lung tissues (Figure 4C). The increased levels of IL-12 expression in dendritic cells and B cells in lung tissue may also account for the preferentially presence of IFN-γ^+ cells in lung tissue compared to dLNs. To ascertain the cellular localization of IL-12 in situ, we carried out immunofluorescence of lung dLNs at day 9 post influenza infection. Consistent with the flow staining, there was little IL-12 expression in B cell zone, especially PNA$^+$ GC areas. We found IL-12 expression mainly localized at the T cell zone or T-B border regions, indicating that IL-12 likely functions outside GCs (Figure 4D).

To investigate the roles of IL-12 in the induction of IFN-γ^+ Tfh cells, we added IL-12 into Tfh cell *in vitro* differentiation cultures. The IFN-γ^+Bcl6$^+$ cells were only observed in Tfh (IL-6$^+$ IL-21) cultures with IL-12, but not in either Th1 (IL-12) or Tfh (IL-6$^+$ IL-21) culture conditions (Figure S2A and B in Supporting Information). Moreover, a relatively low concentration of IL-12 induced even more IFN-γ^+Bcl6$^+$ cells compared to higher concentrations (Figure S2A and B in Supporting Information). Although IL-12 levels did not affect the expression of Bcl6, the presence of IL-6 and IL-21 interfered with the production of IFN-γ in Tfh cells compared to Th1 cells (Figure S2B in Supporting Information). Interestingly, IL-12 promoted the development of IFN-γ^+Bcl6$^+$ cells *in vitro* at early time points (0–24 h), but not late stage (48–72 h) after T cell activation (Figure S2C–E in Supporting Information).

The above results suggest a role for IL-12 in the induction of IFN-γ^+Bcl6$^+$ Tfh cells. To further investigate the functional importance of IL-12 *in vivo*, we infected *Il12b*$^{-/-}$ mice with influenza virus and found that the body weights of the knockout (KO) mice showed a more severe reduction from day 5 to 9 during influenza infection (Figure 4E). Consistently, the virus clearance in lung tissues was defective in the absence of IL-12 (Figure 4F). GC B cell percentages and cell numbers as well as Tfh cell percentages were significantly decreased in the *Il12b*$^{-/-}$ group (Figure 4G). The percentage of IFN-γ^+Bcl6$^+$ double-positive cells among total CD4$^+$CD44$^+$ cells was also greatly reduced in *Il12b*$^{-/-}$ mice (Figure 4H). Meanwhile, total IFN-γ^+ CD4 T cell percentages were also sharply decreased in the KO mice, although IFN-γ^-Bcl6$^+$ CD4$^+$ T cells were not significantly changed (Figure 4H), indicating that, among Tfh cells, the IFN-γ^+ subpopulation was selectively impacted as a result of IL-12 deficiency. Moreover, virus-specific IgG, especially IgG2c was decreased as a result of the deficiency of IL-12 (Figure 4I).

IFN-γ^+ and IFN-γ^- Tfh cells develop independently during viral infection

To further understand the ontogeny of IFN-γ^+ Tfh cells, we utilized an *Ifng*^{cre} mouse that we recently constructed (unpublished data) and generated an *Ifng*^{cre}:*R26*^{YFP} fate-mapping mouse which IFN-γ expressed cells will continuously express YFP. Similar to the *Ifng* reporter mouse, approximately 20% of Tfh cells generated in influenza-infected *Ifng*^{cre}:*R26*^{YFP} mice were found to be YFP$^+$ (Figure 5A), suggesting that, in this model, IFN-γ^- Tfh cells were not generated from an IFN-γ^+ precursor. YFP$^+$ Tfh cells were not present in KLH or SEA immunized mice (Figure 5A). Unexpectedly, we observed that 10%–15% Tfh cells were YFP$^+$ in Peyer's patches, however, such population were not observed in the

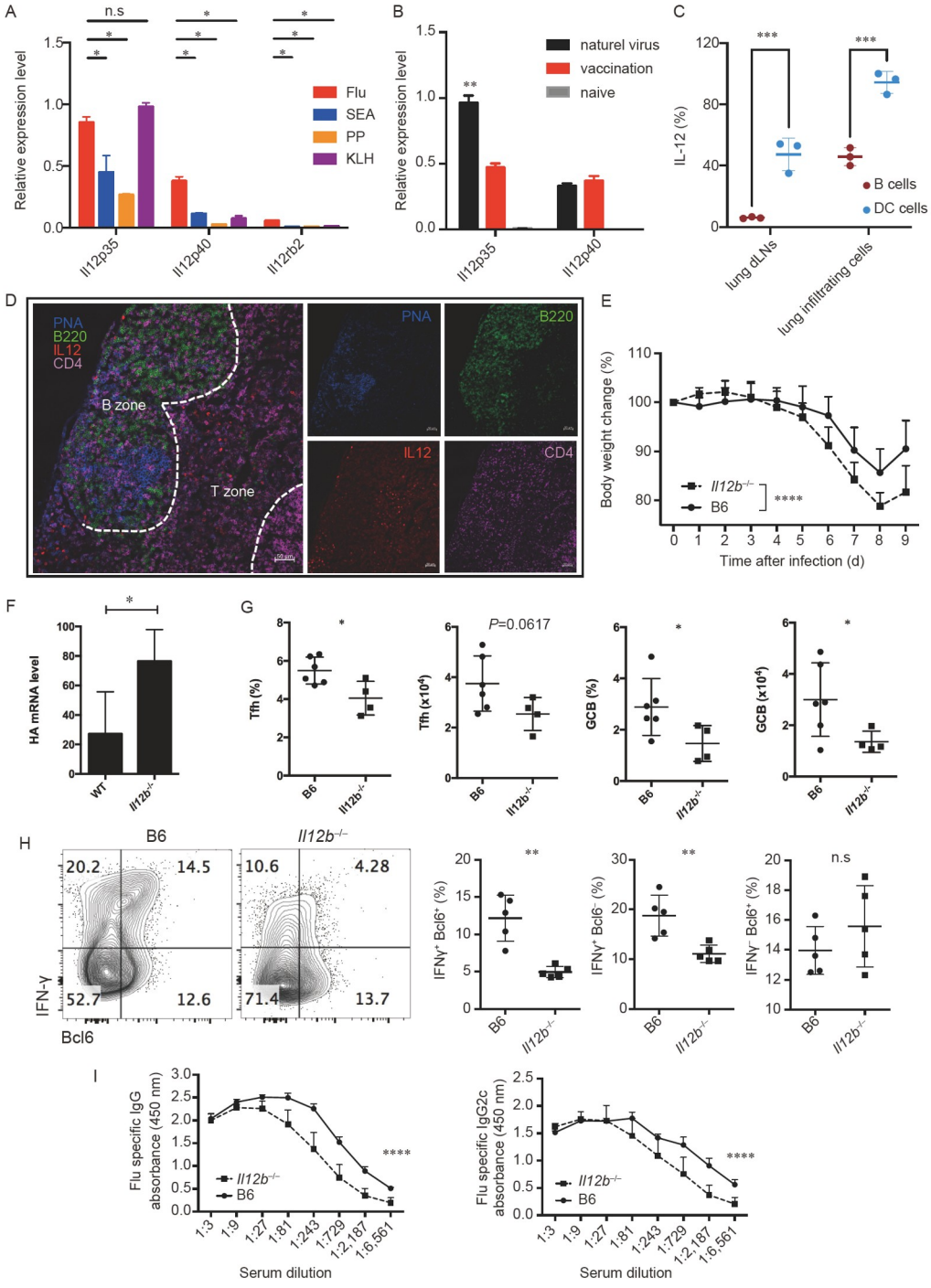

Figure 4 IL-12 regulates the induction of IFN-γ$^+$ Tfh cells during influenza infection. A, Expression of indicated genes in whole tissues from Peyer's patches of C57BL/6 mice at steady state or from the draining lymph nodes in mice infected with H1N1 PR8 virus or immunized with KLH or SEA proteins, respectively. B, Expression of indicated genes in lung draining lymph nodes in naïve C57BL/6 mice and mice infected with live H1N1 PR8 virus or immunized with chemical-inactivated influenza virus. C, Statistical analysis of IL-12 expression in B220$^+$ B cells or CD11c$^+$MHCII$^+$B220$^-$ dendritic cells in lung dLNs or lung-infiltrating cells from influenza infected B6 mice at day 9 post infection. D, Representative immunofluorescence images of PNA (blue), B220 (green), IL-12 (red), CD4 (violet) staining in the frozen sections of lung dLNs from influenza infected B6 mice. E–I, WT and *Il12b*$^{-/-}$ mice infected intranasally with 0.1 LD_{50} of H1N1 PR8 influenza virus and sacrificed for analysis at day 9 post infection. E, Body weight changes were monitored daily. F, Virus titers in lung tissues of WT and *Il12b*$^{-/-}$ mice assessed by hemagglutinin (HA) gene expression using quantitative RT-PCR. G, Percentages and absolute cell numbers of CXCR5$^+$Bcl6$^+$ Tfh cells and GL7$^+$CD95$^+$ GC B cells in lung draining lymph nodes of WT and *Il12b*$^{-/-}$ mice. H, Representative flow images (left) of IFN-γ and Bcl6 reporter expression in CD4$^+$CD44$^+$ cells of lung draining lymph nodes and statistical analysis (right) of IFN-γ$^+$Bcl6$^+$ cells, total IFN-γ$^+$Bcl6$^-$ cells and IFN-γ$^-$Bcl6$^+$ cells percentages in activated CD4$^+$ T cells. I, The amounts of virus-specific serum immunoglobulins from influenza infected B6 and *Il12*$^{-/-}$ mice were measured by ELISA. Data above are representatives of two or three independent experiments. Data of figure A, B, G, H are shown as mean±SD; two-tailed *t*-test; *, P<0.05; **, P<0.01; ***, P<0.001; ****, P<0.0001; n.s, no significance. Data of figure E, I are shown as mean+SD; two-way ANOVA; ****, P<0.0001.

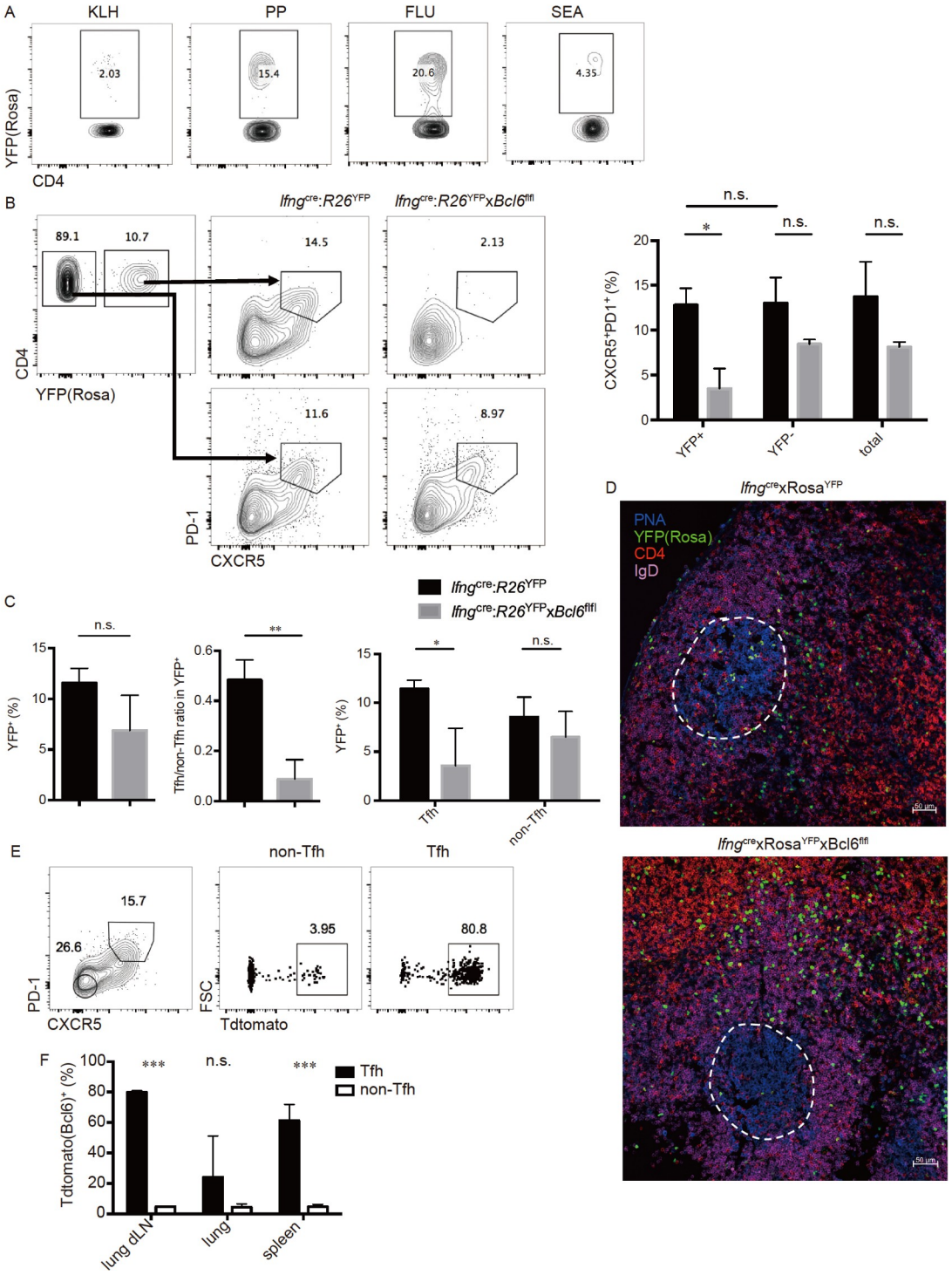

Figure 5 IFN-γ^+ Tfh cells and IFN-γ^- Tfh cells go through distinct development pathways. A, Representative YFP expression in Tfh cells from Peyer's patches at steady state, as well as dLNs in KLH immunized, H1N1 PR8 infected and SEA immunized *Ifng*^{cre}:*R26*^{YFP} fate-mapping mice. B–F, *Ifng*^{cre}:*R26*^{YFP}, *Ifng*^{cre}:*R26*^{YFP}×*Bcl6*^{fifl} mice or *Bcl6*^{CreERT2}:*R26*^{Tdtomato} mice were infected intranasally with 0.1 LD_{50} of H1N1 PR8 influenza virus, sacrificed on day 9 post infection and the lung draining lymph nodes were isolated for further analysis. B, Representative flow staining (left) and statistical analysis (right) of Tfh cells (CXCR5$^+$PD1$^+$) in YFP$^+$ and YFP$^-$ cells in the draining lymph nodes. C, Statistical analysis of percentages of total YFP$^+$ cells in CD4$^+$CD44^{hi} cells (left) and YFP$^+$ cells in Tfh cells and non-Tfh cells (right) in the draining lymph nodes. The ratio of Tfh cells versus non-Tfh cells in total YFP$^+$CD4$^+$CD44^{hi} cells in the draining lymph nodes (middle). D, Immunofluorescence staining of PNA (blue), YFP (green) and CD4 (Red), IgD (violet) in the frozen section of lung draining lymph nodes. E, *Bcl6*^{CreERT2}:*R26*^{Tdtomato} mice were treated with tamoxifen at day 3, 5 and 7 post influenza infection, tdTomato expressions were analyzed in Tfh cells (CD4$^+$CD44^{hi}CXCR5^{hi}PD1^{hi}) and non-Tfh (CD4$^+$CD44^{hi}CXCR5$^-$PD1$^-$) cells from lung dLNs of *Bcl6*^{CreERT2}:*R26*^{Tdtomato} mice. F, Statistical analysis of tdTomato expressions in Tfh cells and non-Tfh cells at lung dLNs, lung infiltrating cells and spleens of *Bcl6*^{CreERT2}:*R26*^{Tdtomato} mice. Data shown above are a representative of two independent experiments. Data are shown as mean±SD; two-tailed *t*-test; *, $P<0.05$; **, $P<0.01$; ***, $P<0.001$; n.s, no significance.

IFN-γ reporter mice which indicated that these cells had previously expressed IFN-γ, but lost the expression of IFN-γ at the time of detection (Figures 2E and 5A). Since the frequencies of Tfh, GC B, and total IFN-γ^+ CD4 T cells in Peyer's patches were not affected in the conditional *Bcl6* knockout mice at steady state, this IFN-γ-expressed fraction of Tfh cells in Peyer's patches do not influence the homeostasis (Figure S3 in Supporting Information).

At day 9 post influenza infection of *Ifng*^{cre}:*R26*^{YFP} mice, we observed Tfh cell formation in both YFP$^+$ or YFP$^-$ CD4$^+$ T cells at similar percentages (Figure 5B). However, when *Ifng*^{cre}:*R26*^{YFP} were crossed with *Bcl6*^{flfl} mice, Tfh cell formation was almost totally abolished among YFP$^+$CD4$^+$ T cells (Figure 5B). At the same time, the total frequency of IFN-γ-expressing cells (Figure 5C, left) as well as IFN-γ expression in non-Tfh cells were unaffected (Figure 5C, right). However, the Tfh versus non-Tfh ratios in YFP$^+$ cells were severely decreased because of Bcl6 deficiency (Figure 5C, middle). We then carried out immunofluorescence analysis and confirmed the localization of IFN-γ-expressing cells within B cell follicles in wild-type mice, which was not the case in the Bcl6-deficient mice (Figure 5D).

To further investigate the plasticity between Tfh cells and Th1 cells, we generated *Bcl6*^{CreERT2}×*R26*^{tdTomato} fate-mapping mice, in which cells historically expressing *Bcl6* would be marked and continuously express tdTomato. We then infected these mice with influenza. Different from CXCR5$^+$ PD1$^+$ Tfh cells in which the majority of cells expressed tdTomato, non-Tfh cells barely expressed it (Figure 5E), excluding the possibility that Th1 cells were derived from Tfh precursors. Similar results were also found in lung-infiltrating lymphocytes and splenocytes (Figure 5F).

Therefore, we conclude that IFN-γ-expressing Tfh cells generated during influenza infection go through a distinct developmental process compared to IFN-γ^- Tfh cells and also that Th1 cells were not derived from Tfh cells.

Elimination of the IFN-γ^+ Tfh population dampened anti-viral GC response

To assess the function of IFN-γ^+ Tfh cells in viral infection, we used *Bcl6*^{flfl}*Ifng*^{cre} conditional knockout mice which IFN-γ^+ Tfh cells were specifically eliminated without influencing the IFN-γ^- Tfh cell population, thus provides a powerful tool to investigate the functional roles of IFN-γ^+ Tfh cells in anti-viral immunity. After intranasally (i.n.) infected *Bcl6*^{flfl}*Ifng*^{cre} (KO) and *Bcl6*^{flfl} (WT) controls with influenza virus A/Puerto Rico/8 (PR8, H1N1), the KO mice displayed a more severe body weight reduction and delayed recovery compared to WT mice from days 5 to 9 after influenza challenge (Figure 6A). At day 9 post infection (dpi), viral hemagglutinin (HA) mRNA levels in the lung tissues of KO mice were much higher than in control mice (Figure 6B), indicating attenuated virus clearance in the KO mice. Although GC B cell as well as Tfh cell and the total IFN-γ^+ cell percentages showed no obvious difference between the two groups, the absolute number of GC B cells in lung draining lymph nodes was lower in the KO mice (Figure 6D). Also, the IgG2c$^+$ GC B cell percentages were substantially decreased as a result of *Bcl6* deletion (Figure 6E), while the IgG1$^+$ cells had no obvious change (Figure 6E). Consistently, though influenza virus-specific IgG1 antibodies had mild differences, virus-specific IgG2c antibodies were decreased in KO mice (Figure 6F), indicating the specific role of IFN-γ^+ cells in modulating IgG2 class switching. *In vitro* co-culture assay also indicated that IFN-γ^+ Tfh cells promote GC B cell differentiation and IgG2c class switching (data not shown). Moreover, an *in vitro* virus neutralizing assay revealed that the generation of neutralizing antibodies against influenza virus was decreased in the absence of IFN-γ^+ Tfh cells (Figure 6C).

Thus, we concluded that IFN-γ^+ Tfh cells are critical for proper humoral immune responses during influenza virus infection, especially mediating anti-viral antibody production and IgG2 class switching in GC. Loss of IFN-γ^+ Tfh cells results in increased susceptibility to influenza virus infection and defects in virus clearance. These results further support earlier work using Zika virus (Liang et al., 2019).

DISCUSSION

In this study, we have systemically defined diverse transcriptional profiles of Tfh cells in the context of different types of immune responses. Influenza infection specifically induces an IFN-γ-expressing Tfh cell type, that is transcriptionally and phenotypically distinct from conventional Tfh cells.

Through transcriptomic profiling of Bcl6-expressing GC-Tfh cells derived from different models, we observed a robust gene expression signature module of GC-Tfh cells apart from *Bcl6*, the lineage-defining factor, in a wide variety of immune responses. The stable expression of these genes is critical for Tfh cell generation and function, but unlikely associates with a particular type of immune response. This cluster of genes could offer hints for the construction of a Tfh cell transcriptional regulation network, which so far remains unclear. In addition to these common genes, we observed the existence of gene clusters associated with immune context-dependent Tfh cell polarization. Bioinformatic analysis identified numerous genes differentially expressed among Tfh cells derived from different immune responses. Particularly, the expression of IFN-γ or IL-4 is not restricted to specific antigens, but rather reflects the type of immune response. These specific Tfh types do not exist at the steady state, but only emerge in response to certain kinds of

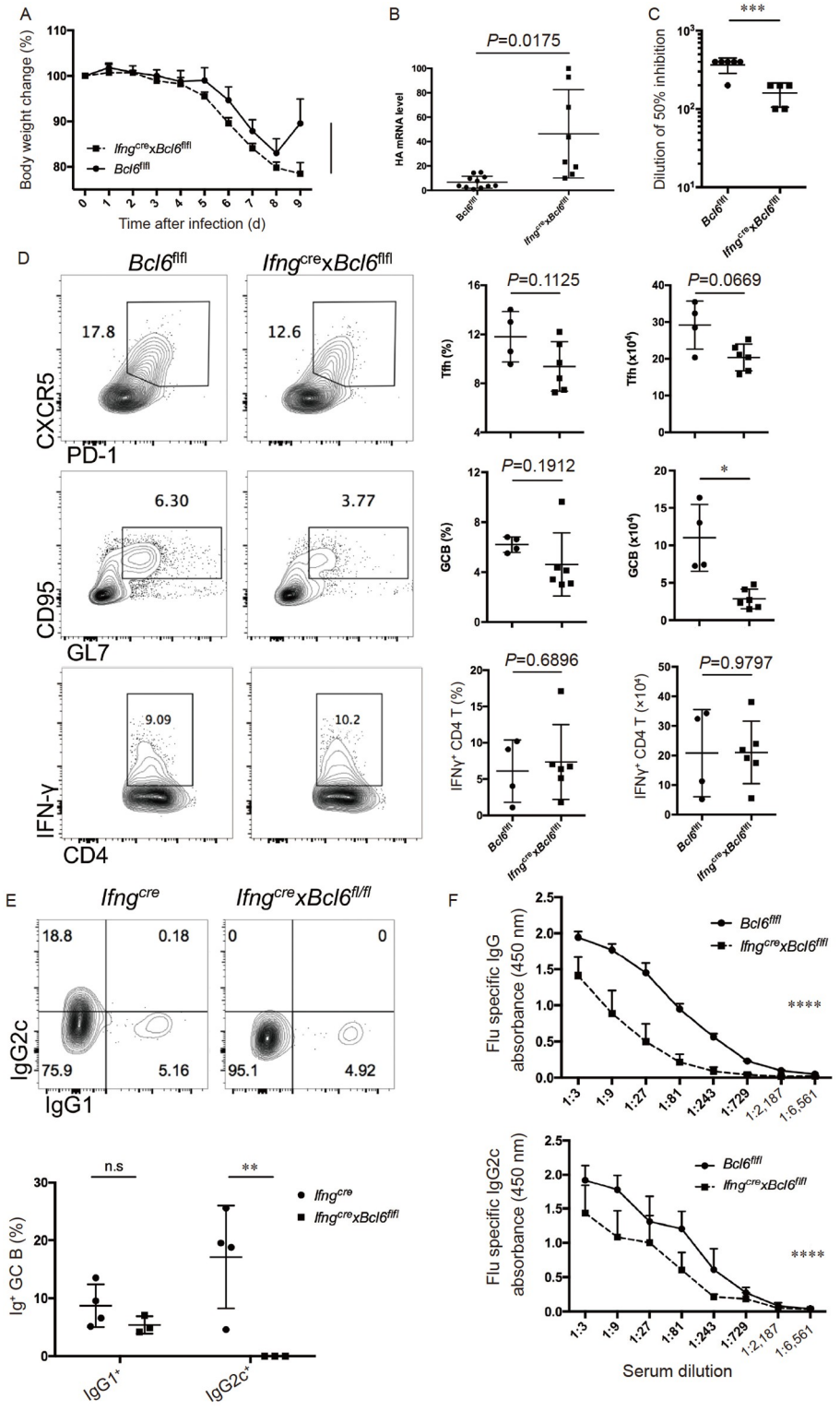

Figure 6 Elimination of IFN-γ^+ Tfh population dampens anti-viral GC responses. *Bcl6*$^{fl/fl}$ (WT) and *Ifng*^{cre}×*Bcl6*$^{fl/fl}$ (KO) mice infected intranasally with 0.1 LD_{50} of H1N1 PR8 influenza virus and sacrificed for analysis 9 d later. A, Body weight changes of *Bcl6*$^{fl/fl}$ (WT) and *Ifng*^{cre}×*Bcl6*$^{fl/fl}$ (KO) mice were monitored daily during virus infection. B, Virus titers in lung tissues as determined by HA gene expression. C, Neutralizing ability of the sera from virus infected WT and KO mice, evaluated as serum dilution values giving 50% of inhibition of viral load in the H1N1 PR8-infected MDCK cells. D, Representative flow images and statistical analysis of Tfh cells (upper), GC B cells (middle) and total IFN-γ^+ CD4 T cells (bottom) in draining lymph nodes of virus infected WT and KO mice. E, Representative flow images (upper) and statistical analysis (bottom) of IgG1$^+$ or IgG2c$^+$ GC B cells in virus infected *Ifng*^{cre} (WT) and *Ifng*^{cre}×*Bcl6*$^{fl/fl}$ (KO) mice. F, The amounts of virus-specific serum immunoglobulins measured by ELISA. Data above are a representative of two or three independent experiments. Data of figure B, C, D, E are shown as mean±SD; two-tailed *t*-test; *, $P<0.05$; **, $P<0.01$; ***, $P<0.001$; ****, $P<0.0001$; n.s, no significance. Data of figure A, F are shown as mean+SD; two-way ANOVA; ****, $P<0.0001$.

infection or innate stimuli. Even at the same anatomic locations, different immune responses still induced differential Tfh responses, largely dependent on the innate signals. The expression of *Ifng* by Tfh cells is closely associated with intracellular viral or bacterial infection, but not in the response to helminth antigens or commensal bacteria in the intestinal microenvironment. The major mechanism for generation of IFN-γ-expressing Tfh cells in bacterial and viral infection is likely the similar immune recognition mechanisms and the innate immune responses to these pathogens (Akira et al., 2006; Stewart and Cookson, 2016). However, anatomic locations may be an important factor in regulation of Tfh cell differentiation. The spatial localization likely restricts certain kind of immune environment and cellular composition which may promote specific Tfh response (Zhang et al., 2021).

Our results revealed that only a fraction of Tfh cells during influenza virus infection expressed IFN-γ. Transcriptional analysis indicated differential gene expression profiles between IFN-γ^+ and IFN-γ^- Tfh subsets. IFN-γ^+ Tfh cells upregulated *Ifng* and *Tbx21* expression during infection, similar to Th1 cells. Previous studies indicated that T-bet is necessary for both Th1 and Tfh cell development in viral infections (Fang et al., 2018; Weinstein et al., 2018). The "ex-T-bet" expression pattern was shown to be critical in the induction of IFN-γ^+ GC-Tfh cells (Fang et al., 2018). Our analysis of *Bcl6* fate-mapping mice has further elucidated the ontogeny of IFN-γ^+ Tfh cells in that they do not generate Bcl6$^-$ Th1 cells. However, such transition was not observed in Th1 cells. Immunofluorescence staining indicated that IL-12 expression mainly localized at T cell zone and T-B border region, but not in B cell follicle of draining lymph nodes. Meanwhile, IL-12 induces IFN-γ^+Bcl6$^+$ cells at first 48 h of T cell activation *in vitro*. Above observations indicated that IL-12 may induce IFN-γ-expressing Tfh precursor cells at T-B border at early phase of immune response. Deficiency of *Bcl6* in IFN-γ-expressing cells resulted in failure of migration of those IFN-γ-expressing Tfh precursor cells into GC areas and maturation into GC-Tfh cells. Thus, influenza infection derived IFN-γ^+ and IFN-γ^- Tfh cells emerged in parallel rather than in sequence. IFN-γ-expressing Tfh cells thus do not represent an intermediate stage of Tfh cell in influenza infection, but rather a subset independent from IFN-γ^- Tfh cells. Our data support the idea of plasticity, but not different developmental stages of Tfh cells during infectious diseases (Crotty, 2018).

IFN-γ-expressing Tfh cells have been also observed by others (Reinhardt et al., 2009; Weinstein et al., 2018). One recent paper calling them IFN-γ-producing Th1-like Tfh cells showed their importance in mediating the serum IgG2c antibody production in ZIKV infection by use of chimeric mouse models (Liang et al., 2019). Our data, consistent with theirs, further show the importance of this unique Tfh cell subset in regulating IgG2 class-switching in GC during viral infection. Specifically, we eliminated IFN-γ^+ Tfh cells during influenza infection without affecting total Tfh cells, but resulting in disappearance of IFN-γ-expressing T cells in germinal centers. Functional data indicated that IFN-γ^+ Tfh cells are critical for the anti-viral antibody response, especially IgG2c$^+$ GC B cell response. Therefore, the interaction of IFN-γ-expressing Tfh cells with GC B cells inside germinal center are critical for isotype switching. These results highlight the importance of IFN-γ^+ Tfh cells in the production of appropriate antibody isotypes and host defense against pathogens.

Innate signals are important in shaping effector T cell generation. Here, we found that IL-12 selectively regulated the development of IFN-γ^+Bcl6$^+$, but not IFN-γ^-Bcl6$^+$ cells during influenza infection. IL-12 has been shown in several studies to be a powerful cytokine used as vaccine adjuvant to enhance cell-mediated cytotoxicity as well as humoral immunity (Jalah et al., 2012; Marinaro et al., 1999; Okada et al., 2017; Stevceva et al., 2006). Given that induction of IFN-γ^+ Tfh cells and IL-12 production were both decreased in mice receiving an inactivated influenza virus vaccine, a strategy to enhance IL-12 signaling should be beneficial in future vaccine design to induce protective humoral immune responses against influenza virus.

Overall, our current work demonstrates adaptive Tfh cell plasticity in response to pathogen infection. Our analysis of IFN-γ^+ Tfh cells generated during influenza virus infection revealed their unique differentiation and regulatory functions. These cells are vital in GC response against viral infection, a finding that has important implications in the future design of anti-viral vaccines.

MATERIALS AND METHODS

Mice

The *Bcl6*^{RFP} and *Bcl6*^{flfl} mice were generated previously (Liu et al., 2012; Liu et al., 2016) and have backcrossed with C57BL/6 mice for at least 8 times. The *Bcl6*^{RFP}mice were crossed with *Foxp3*^{GFP} (Lin et al., 2007) or *Ifng*^{YFP} (Reinhardt et al., 2009) mice in order to generate *Bcl6*^{RFP}×*Foxp3*^{GFP} or *Bcl6*^{RFP}×*Ifng*^{YFP} double reporter mice. The *Bcl6*^{flfl} mice were crossed with *Ifng*^{cre} or *Ifng*^{cre}:*R26*^{YFP} (unpublished) mice in order to generate *Ifng*^{cre}×*Bcl6*^{flfl} *or* *Ifng*^{cre}:*R26*^{YFP}×*Bcl6*^{flfl} conditional knockout mice. *Il12b*$^{-/-}$ mice were a kind gift from Dr. Junling Liu (Shanghai Jiao Tong University). *Bcl6*^{CreERT2} mice generated in house (unpublished) by inserting P2A-iCreERT2 right before the stop codon of the *Bcl6* gene. The *Bcl6*^{CreERT2} mice were crossed with Rosa26-tdTomato(Ai9) mice in order to generate *Bcl6*^{CreERT2}×*R26*^{tdTomato} mice. All the mice were maintained under specific pathogen free (SPF) conditions in Animal Facility of Tsinghua University. All the animal protocols

used in this study were accredited by the AAALAC and IACUC of Tsinghua University.

Animal model

Infection and vaccination

Influenza virus A/Puerto Rico/8 (PR8, H1N1) was generated by Dr. Hong Tang and his colleague at CAS Key Laboratory of Infection and Immunity. For natural virus infection, the mice were anesthetized and intranasally infected with 0.1 half lethal dose (LD_{50}) of H1N1 PR8 influenza virus, and were sacrificed and analyzed on day 9 post infection. The serum was collected for ELISA assays, and the lung draining lymph nodes were isolated for analyzing T and B lymphocytes. Virus titers were determined by relative amounts of viral RNA in the lung tissues using RT-PCR. For vaccination, the mice were intranasally immunized with virus inactivated with 0.05% formaldehyde, and then sacrificed on day 9 or 14 post immunization.

For *Listeria monocytogenes* infection, the mice were intravenously injected with 10^5 CFU of bacteria per mouse in 200 μL of PBS, and sacrificed and analyzed 8 d post infection.

Immunization

For KLH immunization, the mice were subcutaneously immunized with KLH (100 μg per mouse) mixed with CFA (1 mg mL^{-1}, Sigma-Aldrich, USA) near the base of tail, and sacrificed and analyzed on day 7 post immunization.

For *S. mansoni* soluble egg antigen (SEA) immunization, the mice were subcutaneously immunized with SEA (100 μg per mouse) into rear footpads, and then sacrificed and analyzed on day 14 post immunization. The SEA was a kind gift from Dr. Xiaoping Chen at Shanghai Tongji University.

ESS model induction

The ESS model was established by immunizing the mice with mouse salivary gland (SG) proteins as described before with minor modifications (Lin et al., 2015). Briefly, the bilateral salivary gland from mice was collected for homogenization in 1× PBS, the supernatant was collected by centrifugation and the containing soluble SG protein was quantified by BCA assay. The mice were subcutaneously immunized with SG proteins (1 mg per mouse) emulsified in CFA (5 mg mL^{-1}, Sigma-Aldrich) on the neck and then boosted with SG proteins (0.25 mg per mouse) emulsified in Freund's incomplete adjuvant (Sigma-Aldrich) on day 14 after initial immunization. The mice were sacrificed and analyzed at week 5 after initial immunization.

Flow cytometry and cell sorting

For surface staining, cells were first incubated with anti-CD4 (eBioscience, USA), anti-CD44 (BioLegend, USA), biotinylated anti-CXCR5 (BD, USA), followed by streptavidin-BV421 (BioLegend), anti-B220 (eBioscience), anti-PD1 (eBioscience), anti-CD19 (BD), anti-IgD (BioLegend), anti-GL7 (eBioscience), anti-CD95 (eBioscience) staining. Dead cells were excluded by cell viability dye staining (Fixable viability dye eF505, eBioscience).

For intracellular staining, cells were fixed and permeabilized with the Foxp3 transcription factor staining buffer kit (eBioscience), followed by incubation with anti-IFN-γ (BD/eBioscience), anti-BCL6 (BD), anti-IgG1 (BD), anti-IgG2c (Bethyl Laboratories, USA). For intracellular cytokine staining, cells were first stimulated with PMA and ionomycin in the presence of Brefeldin A (Golgiplug, BD) for 5 h prior staining. Cells were analyzed on LSRFortessa (BD) flow cytometer and analyzed using FlowJo.

For cell sorting, cells were sorted on FACSAria (BD) cell sorter with indicated surface marker staining.

RNA-sequencing and Bioinformatics analysis

All samples for RNA-sequencing are followed the same procedure. Total RNA were extracted using RNeasy Micro Kit (QIAGEN, Germany). The quality of the extract RNA was analyzed on Agilent 2100 Bioanalyzer (Agilent, USA). cDNA synthesis and amplification were conducted using SMARTer Ultra Low Input RNA kit (Clontech laboratories, USA). The libraries were generated using Low Input Library Prep Kit (Clontech laboratories). The RNA-sequencing were performed on Hiseq4000 platform (BGI, Shenzhen, China).

Low quality reads and adaptor sequences were removed by Trim Galore v0.4.4. The clean reads were aligned to mm10 by bowtie2 with default parameter, and uniquely mapping reads were summarized by FeatureCounts (from Subread package). Differentially expressed genes were determined using at least 2-fold changes and FDR adjusted p-value less than 0.05 by DEseq2. Highly expressed common genes were determined with FPKM>10 and fold changes less than 2 between any groups.

ELISA

96-well plates were first coated with heat-inactivated virus, washed and then incubated with serial dilution of sera at 4°C overnight, to quantify the amounts of influenza specific antibodies. After washing with 1× PBS with 0.5%Tween 20, the plate-bound virus-specific antibodies were detected by using HRP-conjugated anti-mouse IgG, IgG1, IgG2c. In this study, the influenza virus neutralization assay was performed as previously described (Miyauchi et al., 2016).

Real-time PCR

To determine gene expression level, total RNA was extracted

with Trizol reagent (Invitrogen, USA), and cDNA was synthesized by using SuperScript III Reverse Transcriptase Kit (Thermo Fischer Scientific, USA), and quantified by real time PCR using SYBR real-time kit (Bio-Rad Laboratories, USA). The housekeeping gene *Actb* was used as the internal control for normalizing gene expression.

Immunofluorescence

Tissues were isolated and fixed in 4% paraformaldehyde, then sliced to 6 μm. The frozen sections were stained overnight at 4°C with primary antibodies: biotinylated anti-PNA (Vector lab, USA), anti-IgD (BioLegend). The sections were then incubated with streptavidin-BV421 (BioLegend) at 37 for 2 h. The images were acquired by confocal microscope LSM 780 (Zeiss, Germany) and processed using ZEN imaging software (Zeiss).

T cell *in vitro* differentiation

Naïve CD4 T ($CD4^+CD25^-CD62L^{hi}CD44^{low}$) cells from indicated mice were sorted and cultured with plate-bound anti-CD3 (8 μg mL^{-1}) and anti-CD28 (8 μg mL^{-1}) under following conditions: (i) neutral condition (Th0), anti-IL-2 (10 μg mL^{-1}), anti-IL4 (10 μg mL^{-1}) and anti-TGFβ (5 μg mL^{-1}) in complete RPMI 1640 medium; (ii) Tfh-like condition, Th0 condition plus mIL-6 (20 ng mL^{-1}) and mIL-21 (10 ng mL^{-1}); (iii) Th1 condition, Th0 condition plus mIL-12 (10 ng mL^{-1}). When indicated, mIL-12 were added at 20, 10 or 5 ng mL^{-1} in Tfh-like culture condition for high, middle, low concentrations respectively. Cells were analyzed at 72 h post initial culture.

Statistical analysis

The statistics were performed with two-tail unpaired Student's *t*-test or two-way ANOVA (Graphpad Prism 6), when indicated. Differences with *P*-value<0.05 were considered significant: *, $P<0.05$; **, $P<0.01$; ***, $P<0.001$; n.s, no significant difference.

Data and code availability

Gene expression omnibus: RNA-seq data have been deposited under accession code GSE166248.

Compliance and ethics *The author(s) declare that they have no conflict of interest. All the animal related experiments were performed under the animal welfare policy.*

Acknowledgements *This work was supported in part by the National Natural Science Foundation of China (31630022, 31821003, 31991170 and 31600718) and Beijing Municipal Science and Technology Commission (Z181100001318007 and Z171100000417005). We thank Dr. Junling Liu for providing Il12b$^{-/-}$ mice, Dr. Xiaoping Chen for providing the SEA reagent, and the Tsinghua University Institute for Immunology Core facility for FACS sorting.*

References

Akira, S., Uematsu, S., and Takeuchi, O. (2006). Pathogen recognition and innate immunity. Cell 124, 783–801.

Ansel, K.M., McHeyzer-Williams, L.J., Ngo, V.N., McHeyzer-Williams, M.G., and Cyster, J.G. (1999). *In vivo*-activated CD4 T cells upregulate CXC chemokine receptor 5 and reprogram their response to lymphoid chemokines. J Exp Med 190, 1123–1134.

Bentebibel, S.E., Lopez, S., Obermoser, G., Schmitt, N., Mueller, C., Harrod, C., Flano, E., Mejias, A., Albrecht, R.A., Blankenship, D., et al. (2013). Induction of $ICOS^+$ $CXCR3^+$ $CXCR5^+$ T_H cells correlates with antibody responses to influenza vaccination. Sci Transl Med 5.

Breitfeld, D., Ohl, L., Kremmer, E., Ellwart, J., Sallusto, F., Lipp, M., and Förster, R. (2000). Follicular B helper T cells express CXC chemokine receptor 5, localize to B cell follicles, and support immunoglobulin production. J Exp Med 192, 1545–1552.

Coutelier, J.P., van der Logt, J.T., Heessen, F.W., Warnier, G., and Van Snick, J. (1987). IgG2a restriction of murine antibodies elicited by viral infections. J Exp Med 165, 64–69.

Crotty, S. (2018). Do memory CD4 T cells keep their cell-type programming: plasticity versus fate commitment? Complexities of interpretation due to the heterogeneity of memory CD4 T cells, including T follicular helper cells. Cold Spring Harb Perspect Biol 10, a032102.

Crotty, S. (2019). T follicular helper cell biology: a decade of discovery and diseases. Immunity 50, 1132–1148.

Fang, D., Cui, K., Mao, K., Hu, G., Li, R., Zheng, M., Riteau, N., Reiner, S. L., Sher, A., Zhao, K., et al. (2018). Transient T-bet expression functionally specifies a distinct T follicular helper subset. J Exp Med 215, 2705–2714.

Flannery, B., Chung, J.R., Monto, A.S., Martin, E.T., Belongia, E.A., McLean, H.Q., Gaglani, M., Murthy, K., Zimmerman, R.K., Nowalk, M.P., et al. (2019). Influenza vaccine effectiveness in the United States during the 2016–2017 season. Clin Infect Dis 68, 1798–1806.

Fontenot, J.D., Rasmussen, J.P., Williams, L.M., Dooley, J.L., Farr, A.G., and Rudensky, A.Y. (2005). Regulatory T cell lineage specification by the forkhead transcription factor Foxp3. Immunity 22, 329–341.

Glatman Zaretsky, A., Taylor, J.J., King, I.L., Marshall, F.A., Mohrs, M., and Pearce, E.J. (2009). T follicular helper cells differentiate from Th2 cells in response to helminth antigens. J Exp Med 206, 991–999.

Goodwin, K., Viboud, C., and Simonsen, L. (2006). Antibody response to influenza vaccination in the elderly: a quantitative review. Vaccine 24, 1159–1169.

Gowthaman, U., Chen, J.S., Zhang, B., Flynn, W.F., Lu, Y., Song, W., Joseph, J., Gertie, J.A., Xu, L., Collet, M.A., et al. (2019). Identification of a T follicular helper cell subset that drives anaphylactic IgE. Science 365.

Huber, V.C., McKeon, R.M., Brackin, M.N., Miller, L.A., Keating, R., Brown, S.A., Makarova, N., Perez, D.R., Macdonald, G.H., and McCullers, J.A. (2006). Distinct contributions of vaccine-induced immunoglobulin G1 (IgG1) and IgG2a antibodies to protective immunity against influenza. Clin Vaccine Immunol 13, 981–990.

Jalah, R., Patel, V., Kulkarni, V., Rosati, M., Alicea, C., Ganneru, B., von Gegerfelt, A., Huang, W., Guan, Y., Broderick, K.E., et al. (2012). IL-12 DNA as molecular vaccine adjuvant increases the cytotoxic T cell responses and breadth of humoral immune responses in SIV DNA vaccinated macaques. Hum Vaccines Immunother 8, 1620–1629.

Johnston, R.J., Poholek, A.C., DiToro, D., Yusuf, I., Eto, D., Barnett, B., Dent, A.L., Craft, J., and Crotty, S. (2009). Bcl6 and Blimp-1 are reciprocal and antagonistic regulators of T follicular helper cell differentiation. Science 325, 1006–1010.

Kim, C.H., Rott, L.S., Clark-Lewis, I., Campbell, D.J., Wu, L., and Butcher, E.C. (2001). Subspecialization of $CXCR5^+$ T cells: B helper activity is focused in a germinal center-localized subset of $CXCR5^+$ T

cells. J Exp Med 193, 1373–1382.
King, C., Tangye, S.G., and Mackay, C.R. (2008). T follicular helper (T_{FH}) cells in normal and dysregulated immune responses. Annu Rev Immunol 26, 741–766.
King, I.L., and Mohrs, M. (2009). IL-4–producing CD4+ T cells in reactive lymph nodes during helminth infection are T follicular helper cells. J Exp Med 206, 1001–1007.
Liang, H., Tang, J., Liu, Z., Liu, Y., Huang, Y., Xu, Y., Hao, P., Yin, Z., Zhong, J., Ye, L., et al. (2019). ZIKV infection induces robust Th1-like Tfh cell and long-term protective antibody responses in immunocompetent mice. Nat Commun 10, 3859.
Lin, W., Haribhai, D., Relland, L.M., Truong, N., Carlson, M.R., Williams, C.B., and Chatila, T.A. (2007). Regulatory T cell development in the absence of functional Foxp3. Nat Immunol 8, 359–368.
Lin, X., Rui, K., Deng, J., Tian, J., Wang, X., Wang, S., Ko, K.H., Jiao, Z., Chan, V.S.F., Lau, C.S., et al. (2015). Th17 cells play a critical role in the development of experimental Sjögren's syndrome. Ann Rheum Dis 74, 1302–1310.
Linterman, M.A., Beaton, L., Yu, D., Ramiscal, R.R., Srivastava, M., Hogan, J.J., Verma, N.K., Smyth, M.J., Rigby, R.J., and Vinuesa, C.G. (2010). IL-21 acts directly on B cells to regulate Bcl-6 expression and germinal center responses. J Exp Med 207, 353–363.
Liu, X., Yan, X., Zhong, B., Nurieva, R.I., Wang, A., Wang, X., Martin-Orozco, N., Wang, Y., Chang, S.H., Esplugues, E., et al. (2012). Bcl6 expression specifies the T follicular helper cell program *in vivo*. J Exp Med 209, 1841–1852.
Liu, X., Chen, X., Zhong, B., Wang, A., Wang, X., Chu, F., Nurieva, R.I., Yan, X., Chen, P., van der Flier, L.G., et al. (2014). Transcription factor achaete-scute homologue 2 initiates follicular T-helper-cell development. Nature 507, 513–518.
Liu, X., Lu, H., Chen, T., Nallaparaju, K.C., Yan, X., Tanaka, S., Ichiyama, K., Zhang, X., Zhang, L., Wen, X., et al. (2016). Genome-wide analysis identifies Bcl6-controlled regulatory networks during T follicular helper cell differentiation. Cell Rep 14, 1735–1747.
Ma, C.S., and Deenick, E.K. (2014). Human T follicular helper (Tfh) cells and disease. Immunol Cell Biol 92, 64–71.
Marinaro, M., Boyaka, P.N., Jackson, R.J., Finkelman, F.D., Kiyono, H., Jirillo, E., and McGhee, J.R. (1999). Use of intranasal IL-12 to target predominantly Th1 responses to nasal and Th2 responses to oral vaccines given with cholera toxin. J Immunol 162, 114–121.
Miyauchi, K., Sugimoto-Ishige, A., Harada, Y., Adachi, Y., Usami, Y., Kaji, T., Inoue, K., Hasegawa, H., Watanabe, T., Hijikata, A., et al. (2016). Protective neutralizing influenza antibody response in the absence of T follicular helper cells. Nat Immunol 17, 1447–1458.
Morita, R., Schmitt, N., Bentebibel, S.E., Ranganathan, R., Bourdery, L., Zurawski, G., Foucat, E., Dullaers, M., Oh, S.K., Sabzghabaei, N., et al. (2011). Human blood $CXCR5^{+}CD4^{+}$ T cells are counterparts of T follicular cells and contain specific subsets that differentially support antibody secretion. Immunity 34, 108–121.
Nurieva, R.I., Chung, Y., Hwang, D., Yang, X.O., Kang, H.S., Ma, L., Wang, Y., Watowich, S.S., Jetten, A.M., Tian, Q., et al. (2008). Generation of T follicular helper cells is mediated by interleukin-21 but independent of T helper 1, 2, or 17 cell lineages. Immunity 29, 138–149.
Nurieva, R.I., Chung, Y., Martinez, G.J., Yang, X.O., Tanaka, S., Matskevitch, T.D., Wang, Y.H., and Dong, C. (2009). Bcl6 mediates the development of T follicular helper cells. Science 325, 1001–1005.
Obeng-Adjei, N., Portugal, S., Tran, T.M., Yazew, T.B., Skinner, J., Li, S., Jain, A., Felgner, P.L., Doumbo, O.K., Kayentao, K., et al. (2015). Circulating Th1-cell-type Tfh cells that exhibit impaired B cell help are preferentially activated during acute malaria in children. Cell Rep 13, 425–439.
Okada, M., Kita, Y., Hashimoto, S., Nakatani, H., Nishimastu, S., Kioka, Y., and Takami, Y. (2017). Preclinical study and clinical trial of a novel therapeutic vaccine against multi-drug resistant tuberculosis. Hum Vaccines Immunother 13, 298–305.
Osterholm, M.T., Kelley, N.S., Sommer, A., and Belongia, E.A. (2012). Efficacy and effectiveness of influenza vaccines: a systematic review and meta-analysis. Lancet Infect Dis 12, 36–44.
Ozaki, K., Spolski, R., Feng, C.G., Qi, C.F., Cheng, J., Sher, A., Morse Iii, H.C., Liu, C., Schwartzberg, P.L., and Leonard, W.J. (2002). A critical role for IL-21 in regulating immunoglobulin production. Science 298, 1630–1634.
Park, S.R., Seo, G.Y., Choi, A.J., Stavnezer, J., and Kim, P.H. (2005). Analysis of transforming growth factor-β1-induced Ig germ-line γ2b transcription and its implication for IgA isotype switching. Eur J Immunol 35, 946–956.
Reinhardt, R.L., Liang, H.E., and Locksley, R.M. (2009). Cytokine-secreting follicular T cells shape the antibody repertoire. Nat Immunol 10, 385–393.
Romani, L., Puccetti, P., and Bistoni, F. (1997). Interleukin-12 in infectious diseases. Clin Microbiol Rev 10, 611–636.
Ryg-Cornejo, V., Ioannidis, L.J., Ly, A., Chiu, C.Y., Tellier, J., Hill, D.L., Preston, S.P., Pellegrini, M., Yu, D., Nutt, S.L., et al. (2016). Severe malaria infections impair germinal center responses by inhibiting T follicular helper cell differentiation. Cell Rep 14, 68–81.
Sangster, M.Y., Topham, D.J., D'Costa, S., Cardin, R.D., Marion, T.N., Myers, L.K., and Doherty, P.C. (2000). Analysis of the virus-specific and nonspecific B cell response to a persistent B-lymphotropic gammaherpesvirus. J Immunol 164, 1820–1828.
Schaerli, P., Willimann, K., Lang, A.B., Lipp, M., Loetscher, P., and Moser, B. (2000). CXC chemokine receptor 5 expression defines follicular homing T cells with B cell helper function. J Exp Med 192, 1553–1562.
Schmitt, N., Bentebibel, S.E., and Ueno, H. (2014). Phenotype and functions of memory Tfh cells in human blood. Trends Immunol 35, 436–442.
Shaw, L.A., Bélanger, S., Omilusik, K.D., Cho, S., Scott-Browne, J.P., Nance, J.P., Goulding, J., Lasorella, A., Lu, L.F., Crotty, S., et al. (2016). Id2 reinforces TH1 differentiation and inhibits E2A to repress TFH differentiation. Nat Immunol 17, 834–843.
Snapper, C.M., and Paul, W.E. (1987). Interferon-γ and B cell stimulatory factor-1 reciprocally regulate Ig isotype production. Science 236, 944–947.
Stevceva, L., Moniuszko, M., and Grazia Ferrari, M. (2006). Utilizing IL-12, IL-15 and IL-7 as mucosal vaccine adjuvants. Lett Drug Des Discov 3, 586–592.
Stewart, M.K., and Cookson, B.T. (2016). Evasion and interference: intracellular pathogens modulate caspase-dependent inflammatory responses. Nat Rev Microbiol 14, 346–359.
Suto, A., Nakajima, H., Hirose, K., Suzuki, K., Kagami, S., Seto, Y., Hoshimoto, A., Saito, Y., Foster, D.C., and Iwamoto, I. (2002). Interleukin 21 prevents antigen-induced IgE production by inhibiting germ line Cε transcription of IL-4-stimulated B cells. Blood 100, 4565–4573.
Velu, V., Mylvaganam, G.H., Gangadhara, S., Hong, J.J., Iyer, S.S., Gumber, S., Ibegbu, C.C., Villinger, F., and Amara, R.R. (2016). Induction of Th1-biased T follicular helper (Tfh) cells in lymphoid tissues during chronic simian immunodeficiency virus infection defines functionally distinct germinal center Tfh cells. J Immunol 197, 1832–1842.
Velu, V., Mylvaganam, G., Ibegbu, C., and Amara, R.R. (2018). Tfh1 cells in germinal centers during chronic HIV/SIV infection. Front Immunol 9.
Vinuesa, C.G., Linterman, M.A., Yu, D., and MacLennan, I.C.M. (2016). Follicular helper T cells. Annu Rev Immunol 34, 335–368.
Ward, E.S., and Ghetie, V. (1995). The effector functions of immunoglobulins: implications for therapy. Ther Immunol 19, 77–94.
Weinstein, J.S., Herman, E.I., Lainez, B., Licona-Limón, P., Esplugues, E., Flavell, R., and Craft, J. (2016). TFH cells progressively differentiate to regulate the germinal center response. Nat Immunol 17, 1197–1205.
Weinstein, J.S., Laidlaw, B.J., Lu, Y., Wang, J.K., Schulz, V.P., Li, N., Herman, E.I., Kaech, S.M., Gallagher, P.G., and Craft, J. (2018). STAT4 and T-bet control follicular helper T cell development in viral infections. J Exp Med 215, 337–355.

Wu, L.C., and Zarrin, A.A. (2014). The production and regulation of IgE by the immune system. Nat Rev Immunol 14, 247–259.
Xu, J., Foy, T.M., Laman, J.D., Elliott, E.A., Dunn, J.J., Waldschmidt, T.J., Elsemore, J., Noelle, R.J., and Flavell, R.A. (1994). Mice deficient for the CD40 ligand. Immunity 1, 423–431.
Xu, Z., Zan, H., Pone, E.J., Mai, T., and Casali, P. (2012). Immunoglobulin class-switch DNA recombination: Induction, targeting and beyond. Nat Rev Immunol 12, 517–531.
Yu, D., Rao, S., Tsai, L.M., Lee, S.K., He, Y., Sutcliffe, E.L., Srivastava, M., Linterman, M., Zheng, L., Simpson, N., et al. (2009). The transcriptional repressor Bcl-6 directs T follicular helper cell lineage commitment. Immunity 31, 457–468.
Zhang, J., Wang, Y., Yu, H., Chen, G., Wang, L., Liu, F., Yuan, J., Ni, Q., Xia, X., and Wan, Y. (2021). Mapping the spatial distribution of T cells in repertoire dimension. Mol Immunol 138, 161–171.
Živković, I., Petrović, R., Arsenović-Ranin, N., Petrušić, V., Minić, R., Bufan, B., Popović, O., and Leposavić, G. (2018). Sex bias in mouse humoral immune response to influenza vaccine depends on the vaccine type. Biologicals 52, 18–24.
Zotos, D., Coquet, J.M., Zhang, Y., Light, A., D'Costa, K., Kallies, A., Corcoran, L.M., Godfrey, D.I., Toellner, K.M., Smyth, M.J., et al. (2010). IL-21 regulates germinal center B cell differentiation and proliferation through a B cell-intrinsic mechanism. J Exp Med 207, 365–378.

SUPPORTING INFORMATION

The supporting information is available online at https://doi.org/10.1007/s11427-021-2055-x. The supporting materials are published as submitted, without typesetting or editing. The responsibility for scientific accuracy and content remains entirely with the authors.